Blind Channel Equalization with Amplitude Banded Godard and Sato Algorithms

Muhammad Lutfor Rahman Khan, Mohammed H. Wondimagegnehu and Tetsuya Shimamura
Graduate School of Science and Engineering, Saitama University
255 Shimo-okubo, Sakura-ku, Saitama 338-8570, Japan.
Email: {khan, momy, shima}@sie.ics.saitama-u.ac.jp

Abstract—**The least-mean-squares (LMS) algorithm which updates the filter coefficients by a stochastic gradient descent approach is the most popular adaptive filtering one. In this paper we propose a novel amplitude banded (AB) technique with LMS on Godard (ABGodard) and Sato (ABSato) algorithms for the equalization of communication channels. The non-linear properties of the AB technique with LMS algorithm are inherited into the ABGodard and ABSato algorithms, resulting in an improvement of equalization performance. These properties are validated from a signal separation aspect based on decision boundary. Mean square error (MSE) and bit error rate (BER) are investigated on several communication channel models. Observations on simulations show that the ABGodard and ABSato algorithms provide better performance than the standard Godard and Sato algorithms, respectively, and that the ABSato algorithm is superior to the ABGodard algorithm. As the division number used for the AB technique is increased, the MSE and BER performances of the ABSato algorithm are improved. A parallel structure of the Sato and ABSato algorithms provides a further improvement of the MSE and BER performances.**

Index Terms—**Least-Mean-Squares, Non-linear Adaptive Algorithm, ABGodard Algorithm, ABSato Algorithm, Blind Equalization**

I. INTRODUCTION

The physical channel introduces a distortion to the transmitted signal. To recover the original signal, the principle of channel equalization plays an important role in digital communication systems. To reduce or ideally to eliminate completely the intersymbol interference (ISI) induced by the channel, adaptive equalization [1] is required. Although conventional equalization techniques rely on training sequence based equalization, they suffer from the trade-off between the sequence length and the capacity of the link. To avoid this problem and when the training sequence is not available, blind equalization technique [2] can be used. Thus the blind channel equalization is the great deal of attention for its importance in digital communication systems. The Godard [3] and Sato [4] adaptive algorithms are widely used blind algorithms for equalization of a channel. They are commonly derived based on measuring the output of the channel in case of lacking explicit knowledge of the transmitted sequence.

Blind adaptive equalizers are often composed of two distinct sections: (i) an adaptive filter adapted by linear adaptive algorithm (ii) followed by a non-linear estimator to improve the filter outputs. The improved output of the filter is taken to improve the estimator output in the adaptation process at the next iteration.

In the adaptation process, a linear adaptive least-mean-squares (LMS) algorithm is used for the Godard and Sato equalizers. Due to the linear property of LMS algorithm it can not always select the appropriate tap values for adaptation. We use a non-linear adaptive algorithm which can select the appropriate tap values and improve the performance of the blind equalizer. Recently, Shimamura et.al [5] derived a new non-linear adaptive algorithm, called amplitude banded LMS (ABLMS) algorithm, for training sequence based equalization. The adaptation of the ABLMS algorithm considers the amplitude information of the channel output to select the coefficients of the equalizer as non-linear switching pattern. The ABLMS algorithm exhibits better performance than the conventional LMS algorithm. In this paper, we set out to apply the amplitude banded (AB) technique [6] in blind adaptive algorithm to obtain better performance. Actually, we propose the AB version of the Godard and Sato algorithms. In the proposed amplitude banded Godard (ABGodard) and amplitude banded Sato (ABSato) algorithms, the amplitude information is deployed to select the coefficients to be updated. Based on the amplitude level of the received sequence, the equalizer coefficients are (for each iteration) selected from the elements of the coefficient matrix, and then updated. Since the AB technique itself provides the capability of non-linear classification [7] and the increase of division number of the AB technique enhances its non-linearity [5], thus it is expected that the proposed ABGodard and ABSato algorithms provide better performance than the Godard and Sato algorithms, respectively. The AB versions with blind equalizer are the first in this area and have strong novelty with simulation results in mean square error (MSE) and bit error rate (BER) performances.

This paper is organized as follows. In Section II, the channel model considered in this paper is described and the problem of blind channel equalization is formulated. In Section III, the two proposed algorithms, ABGodard and ABSato algorithms, are described and a performance analysis is made from a signal separation aspect. Section IV shows simulation results. In Section V, we consider the filter structure for the blind equalizer and derive a

Manuscript received February 3, 2009; revised March 25, 2009; accepted May 11, 2009.

parallel structure to provide a performance improvement. Finally, this paper is concluded in Section VI.

II. Channel Model and Blind Equalizer

Through this paper, the channel model assumed is given by

$$u(k) = \sum_{i=0}^{L} h_i x(k-i) + v(k) \tag{1}$$

where $h_o, h_1, ..., h_L$ are the channel coefficients, $u(k)$ is the transmitted sequence, and $v(k)$ is a white Gaussian noise uncorrelated with $x(k)$. The channel output $u(k)$ becomes the input for the equalizer. Figure 1 shows

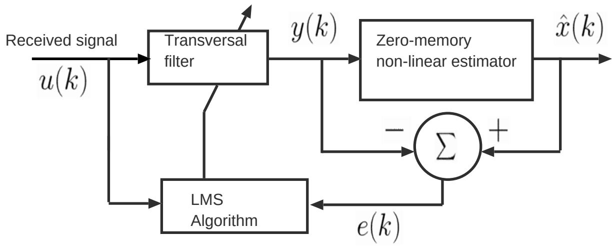

Fig. 1. Block diagram of the blind equalizer

a block diagram of the blind equalizer [8]. In Figure 1, $y(k)$ is the transversal filter output to the equalizer input $u(k)$. $y(k)$ plays a key role in the cost function of blind adaptation. For the Sato algorithm, $y(k)$ is applied to estimate the transmitted sequence $x(k)$ as $\hat{x}(k)$. For most of the blind algorithms, the LMS algorithm can be commonly utilized to update the coefficient vector with the information of the estimation error $e(k)$.

III. AB Blind Algorithm

The two proposed algorithms, ABGodard and ABSato, are described in this section.

A. ABGodard Algorithm

In implementing the ABGodard algorithm, the cost function minimization is considered as the same as that of the Godard algorithm. The cost function of the ABGodard algorithm is

$$J(k) = E[(\mid y(k) \mid^p - R_p)^2] \tag{2}$$

where $y(k)$ is the transversal filter output, p is a positive integer and R_p is a positive real constant defined by

$$R_p = \frac{E[\mid x(k) \mid^{2p}]}{E[\mid x(k) \mid^{p}]} \tag{3}$$

where E denotes expectation. The error signal can be calculated as

$$e(k) = y(k) \mid y(k) \mid^{p-2} (R_p - \mid y(k) \mid^p). \tag{4}$$

For the adaptation of the ABGodard algorithm, a $Q \times M$ coefficient matrix $\mathbf{Z_{abg}}(k)$ is considered, the elements of which are given by $w_{i,j}(k)$, $i = 1, 2, ..., Q$, $j = 1, 2, ..., M$. $\mathbf{Z_{abg}}(k)$ is initialized at $k = 0$ and all other elements are set to zeros considering the initialization condition according to channel characteristics. First element of the matrix is set to unity for minimum phase channel as for initialization. In the adaptation process of the algorithm, the elements of $\mathbf{Z_{abg}}(k)$ are updated as the pattern of switching of the elements to be updated. Among the $Q \times M$ elements of $\mathbf{Z_{abg}}(k)$, only M elements, $w_{r(s),s}(k)$, $s = 1, 2, ..., M$ are selected for each iteration and a coefficient vector, $\mathbf{w_{abg}}(k) = (w_{r(1)1}(k), w_{r(2)2}(k), ..., w_{r(m)m}(k))^T$, where $r(s)$ is an integer and determined on the basis of the amplitude level of each element $u(k-s+1)$ of the input vector $\mathbf{u}(k)$, is formed for $s = 1, 2, ..., M$ as follows:

- if $|u(k-s+1)| \leq A_{max}/Q$, then $r(s) = 1$.
- if $A_{max}/Q < |u(k-s+1)| \leq 2A_{max}/Q$, then $r(s) = 2$.
- if $2A_{max}/Q < |u(k-s+1)| \leq 3A_{max}/Q$, then $r(s) = 3$.
- . . .
- . . .
- if $(Q-1)A_{max}/Q < |u(k-s+1)|$, then $r(s) = Q$.

Here, A_{max} denotes the maximum amplitude of the channel output and Q corresponds to the number of divisions used to partition the amplitude of the channel output. A_{max} should be measured from the received sequence before the equalizer is implemented. Accurate estimation of A_{max} is desired, but slightly inaccurate estimation may be also acceptable. This is because the range of the amplitude corresponding to $r(s) = Q$ is not severely restricted, and occurs with the lowest probability compared with the other range cases. As an example, consider that the equalizer length is M=5 and the input vector is given by

$$\mathbf{u}(k) = [\ 0.35 \quad -0.17 \quad 0.70 \quad 0.55 \quad 0.15\ ]^T.$$

If we consider the division number Q=4, then the 4 by 5 coefficient matrix is prepared as follows :

$$\mathbf{Z_{abg}}(k) = \begin{bmatrix} w_{11}(k) & w_{12}(k) & w_{13}(k) & w_{14}(k) & w_{15}(k) \\ w_{21}(k) & w_{22}(k) & w_{23}(k) & w_{24}(k) & w_{25}(k) \\ w_{31}(k) & w_{32}(k) & w_{33}(k) & w_{34}(k) & w_{35}(k) \\ w_{41}(k) & w_{42}(k) & w_{43}(k) & w_{44}(k) & w_{45}(k) \end{bmatrix}.$$

The value of A_{max} is assumed to be 0.8. Since each element of $\mathbf{u}(k)$ produces $r(1) = 2$, $r(2) = 1$, $r(3) = 4$, $r(4) = 3$, $r(5) = 1$, the coefficient vector $\mathbf{w_{abg}}(k)$ becomes $\mathbf{w_{abg}}(k)$=$[w_{21}(k), w_{12}(k) w_{43}(k), w_{34}(k), w_{15}(k)]^T$. This vector is updated by the Godard algorithm, and then the updated coefficients $w_{21}(k+1), w_{12}(k+1), w_{43}(k+1), w_{34}(k+1), w_{15}(k+1)$ are inserted into the coefficient matrix $\mathbf{Z_{abg}}(k+1)$. For the next iteration, a coefficient vector is again prepared based on the elements of the input and then updated by the Godard algorithm. In such a way all the elements of $\mathbf{Z_{abg}}(k)$ are updated for all input data. For selection of the filter coefficients in such a way at each iteration, the filter provides better output, which helps to estimate more accurate desired signal than that at the previous iteration. At the k^{th} iteration, the adaptive equations for the ABGodard algorithm are given by

$$y(k) = \mathbf{u}(k)^T \mathbf{w_{abg}}(k) \quad (5)$$

$$e(k) = y(k) \mid y(k) \mid^{p-2} (R_p - \mid y(k) \mid^p) \quad (6)$$

$$\mathbf{w_{abg}}(k+1) = \mathbf{w_{abg}}(k) + \mu e(k)\mathbf{u}(k) \quad (7)$$

where μ is the step size and $\mathbf{w_{abg}}(k+1)$ is the coefficient vector.

B. ABSato Algorithm

In implementing the ABSato algorithm, the cost function minimization is considered as the same as that of the Sato algorithm. That is, the ABSato algorithm consists of minimizing a non-convex cost function

$$J(k) = E[(\hat{x}(k) - y(k))^2] \quad (8)$$

where $y(k)$ is the transversal filter output and $\hat{x}(k)$ is an estimate of the transmitted sequence. $\hat{x}(k)$ is given by

$$\hat{x}(k) = \gamma sgn[y(k)] \quad (9)$$

where the function $sgn()$ is the signum function which returns the sign of the argument. $sgn[y(k)]$ is 1 if $y(k)$ is positive, 0 if $y(k)$ is zero and -1 if $y(k)$ is negative. The constant γ sets the gain of the equalizer, which is defined by

$$\gamma = \frac{E[x^2(k)]}{E[|x(k)|]} \quad (10)$$

and the adaptive equations for the ABSato algorithm are given by

$$y(k) = \mathbf{u}(k)^T \mathbf{w_{abs}}(k) \quad (11)$$

$$e(k) = \hat{x}(k) - y(k) = \gamma sgn(y(k)) - y(k) \quad (12)$$

$$\mathbf{w_{abs}}(k+1) = \mathbf{w_{abs}}(k) + \mu e(k)\mathbf{u}(k) \quad (13)$$

where $e(k)$ is the estimation error and $\mathbf{w_{abs}}(k)$ is the coefficient vector.

C. Performance Analysis

Due to the non-linear properties of the AB adaptation (coefficients are selected according to the amplitude level of the equalizer input), the ABSato algorithm provides better performance for convergence and BER. In case of BER, the non-linearity can be explained as follows.

Let us consider the channel whose transfer function is given by

$$Channel1 : H_1(z) = 1.0 + 0.5z^{-1} \quad (14)$$

and the transmitted signal consists of a pseudo-random sequence with values of 1 or -1. For this channel model, a linear transversal equalizer with two taps requires the last two channel output samples $u(k)$ and $u(k-1)$ as the equalizer inputs. All possible samples of these are summarized in Table I as the channel inputs and outputs [9].

TABLE I
CHANNEL INPUTS AND OUTPUTS

$x(k)$	$x(k-1)$	$x(k-2)$	$u(k)$	$u(k-1)$
-1	-1	-1	-1.5	-1.5
-1	-1	1	-1.5	-0.5
-1	1	-1	-0.5	0.5
-1	1	1	-0.5	1.5
1	-1	-1	0.5	-1.5
1	-1	1	0.5	-0.5
1	1	-1	1.5	0.5
1	1	1	1.5	1.5

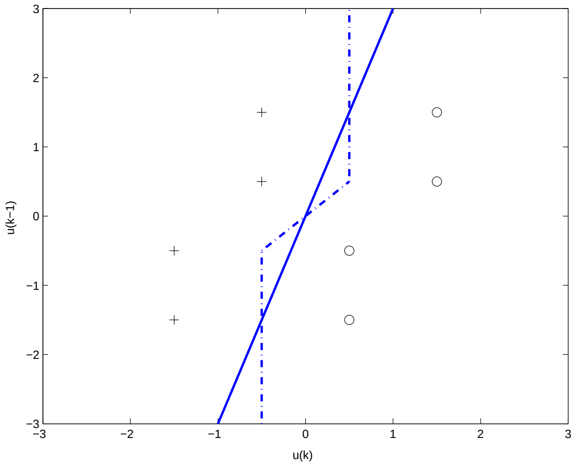

Fig. 2. Channel outputs and decision boundary

If $u(k)/u(k-1)$ plot is used, then the equalizer task is to separate the transmitted sequence by decision boundary as shown in Figure 2. In Figure 2, $\circ$ and $+$ correspond to 1 and -1 transmitted, whose coordinates are obtained from Table I. Ideal separation is obtained by the dash dotted line, which can be realized by non-linear classifiers such as neural networks [9]. A linear equalizer provides only a straight line as shown by the solid line. This case is imperfect particularly in a highly noisy environment, because each transmitted sequence is usually distributed by making a circle in noisy environments on signal plot representation as shown in Figure 2.

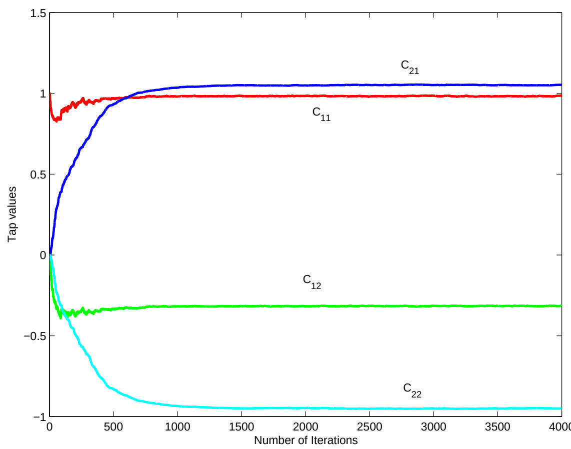

Fig. 3. Convergence of the tap coefficients of the ABSato equalizer for the case $M = 1$ and SNR=40 dB.

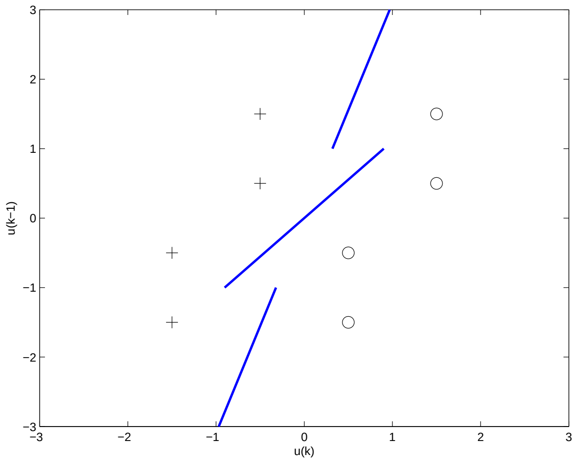

Fig. 4. Decision boundary obtained by the ABSato Equalizer

Figure 3 shows the convergence of the ABSato equalizer coefficients with setting the filter order $M = 1$, division number Q=2, step size μ =0.026 and SNR=40 dB on Channel 1. Due to the blind mode status, the first coefficient C_{11} is initialized with unity. Figure 3 provides C_{11}=0.9854, C_{12}=-0.3164 and C_{21}=1.0531, C_{22}=-0.9500 in convergence. These result in signal separation curves given by

$$u(k-1) = -\frac{C_{11}}{C_{12}} u(k) = 3.11 u(k) \quad (15)$$

for $\mid u(n)\mid \geq$1.0 and $\mid u(n-1)\mid \geq$1.0 and

$$u(k-1) = -\frac{C_{21}}{C_{22}} u(k) = 1.10 u(k) \quad (16)$$

for $0 \leq \mid u(n) \mid \leq 1.0$ and $0 \leq \mid u(n-1)\mid \leq 1.0$, respectively. The above two curves are obtained from the coefficient matrix according to the amplitude banding of the input signal. The resulting curves are plotted in Figure 4. The curves in Figure 4, being the decision boundary, contain discontinuities in the straight line, shape of which is similar with that of the dotted line in Figure 2. This suggests that the ABSato equalizer has the potential of non-linear classification. Due to this non-linear properties, the ABSato algorithm provides better performance than the Sato algorithm.

This type of analysis for the ABSato algorithm is also applicable for the ABGodard algorithm.

IV. Performance Evaluation

To investigate the performances of the ABGodard and ABSato algorithms, simulation experiments were conducted. First of all the channel models whose transfer functions are given by (14) and

$$Channel2 : H_2(z) = 0.5 + 1.0z^{-1} \quad (17)$$

were considered. Channels 1 and 2 are minimum phase and maximum phase, respectively.

Figures 5 and 6 show the MSE convergence plots on Channels 1 and 2, respectively, where the Godard, Sato, ABGodard and ABSato algorithms are compared

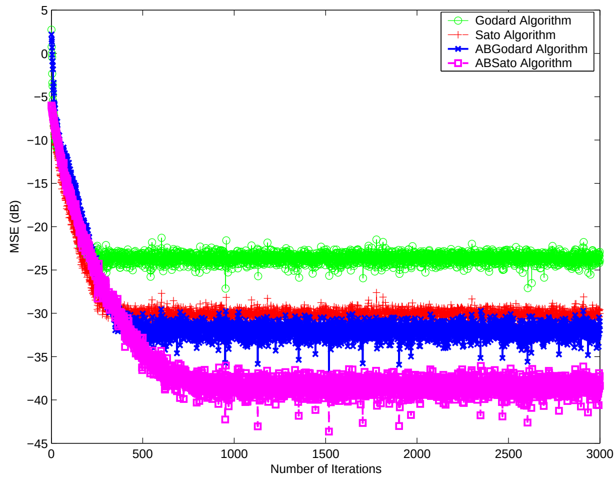

Fig. 5. MSE performance of Godard, Sato, ABGodard and ABSato on Channel 1 with SNR=40 dB

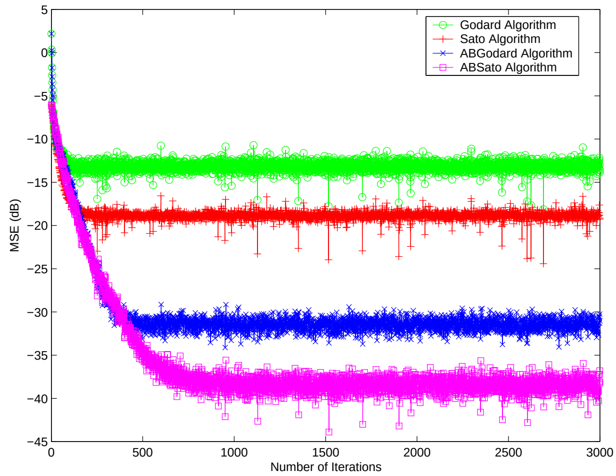

Fig. 6. MSE performance of Godard, Sato, ABGodard and ABSato on Channel 2 with SNR=40 dB

under the conditions of SNR=40 dB, step size μ=0.025, number of division Q=4 and filter order M=4. Each MSE convergence plot is an evaluation of 100 individual runs. Figures 5 and 6 indicate that commonly the AB versions provide better performance, while the ABSato algorithm results in a smaller MSE level in convergence on both channels. According to this result, we decided to select the ABSato algorithm in order to investigate the performance furthermore on other channels whose transfer functions are given by

$$Channel3 : H_3(z) = 1.0 + 2.2z^{-1} + 0.4z^{-2} \quad (18)$$

$$\begin{aligned} Channel4 : H_4(z) &= 0.06 - 0.07z^{-1} + 0.1z^{-2} \\ &- 0.5z^{-3} - 0.9z^{-4} + 1.0z^{-5} \\ &+ 0.3z^{-6} + 0.2z^{-7} + 0.05z^{-8} \\ &+ 0.1z^{-9} \end{aligned} \quad (19)$$

and

$$Channel5 : H_5(z) = h_0(k) + h_1(k)z^{-1} + h_2(k)z^{-2}, \quad (20)$$

respectively. Channels 3 and 4 are non-minimum phase. Channel 5 is a time-variant multipath channel, where the time-variant coefficients, $h_0(k)$, $h_1(k)$ and $h_2(k)$ are generated by passing a Gaussian white noise through a second order Butterworth filter which is designed with a sampling rate of 2400 samples/s. The channel fade rate can be quoted as the 3 dB bandwidth for the Markov process. Commonly, the input sequence is assumed to be a pseudo-random sequence with values of +1 or -1. Channel 5 corresponds to a high frequency (HF) channel model $H_3(z)$ used in [10].

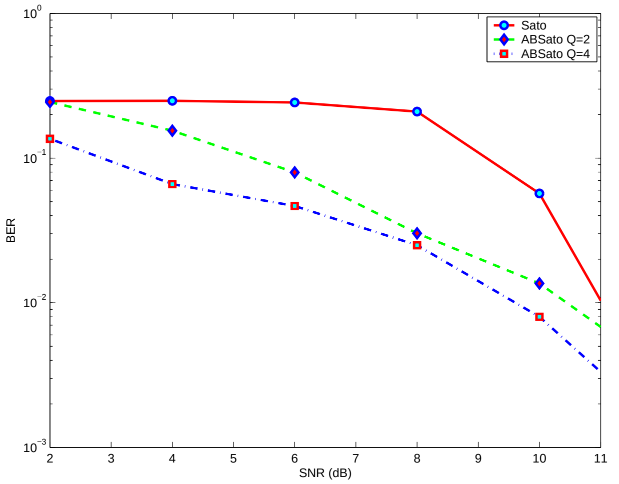

Fig. 7. BER performance of Sato and ABSato on Channel 1

Figure 7 illustrates a BER performance comparison of the Sato and ABSato algorithms on Channel 1, where the step size μ=0.031 and filter order M=6 were used. In Figure 7, the performances of the ABSato algorithm with the division numbers $Q = 2$ and $Q = 4$

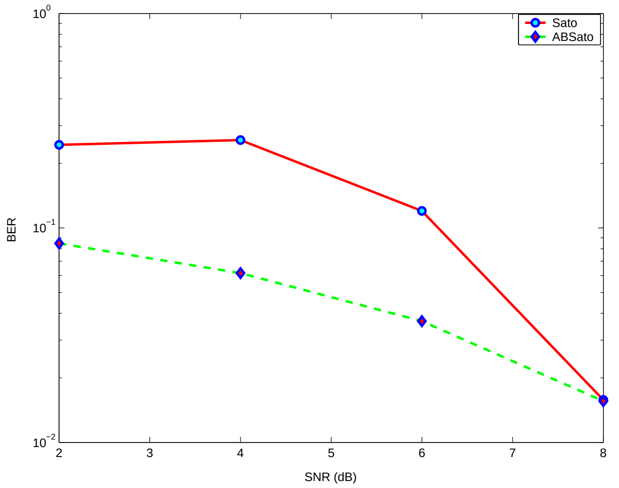

Fig. 8. BER performance of Sato and ABSato on Channel 2

Figure 8 also illustrates BERs of the Sato and ABSato algorithms on Channel 2, where the step size μ=0.021 and filter order M=4 were used and the division number $Q = 2$ was set. Figure 8 again indicates that the ABSato algorithm is better.

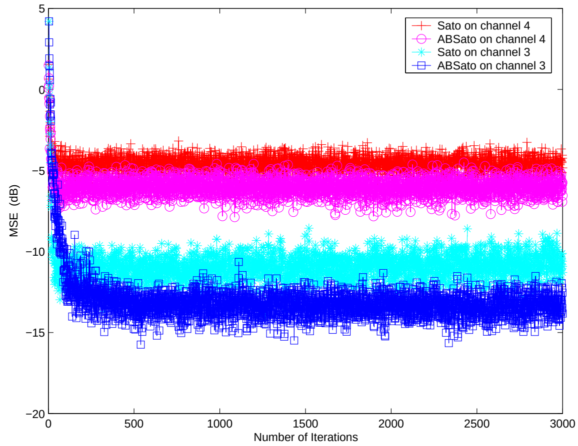

Fig. 9. MSE performance on Channels 3 and 4 with SNR=20 dB

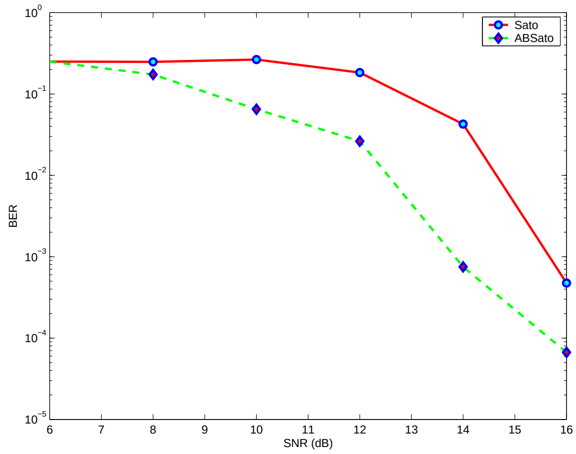

Fig. 10. BER performance of Sato and ABSato on Channel 3

Figure 9 shows the MSE convergence plots of the Sato and ABSato algorithms on Channels 3 and 4 with SNR=20 dB. Figures 10 and 11 illustrate BERs of the Sato and ABSato algorithms on Channels 3 and 4, respectively. Setting $Q = 2$ was commonly used. The step size and filter order were, however, changed in Figures 9, 10 and 11 as $\mu = 0.025$ and $M = 4$ in Figure 9, $\mu = 0.01$ and $M = 8$ in Figure 10 and $\mu = 0.012$ and $M = 11$ in Figure 11. From Figures 9, 10 and 11, it is observed that Channel 4 is more severe for channel equalization than Channel 3, but the ABSato algorithm provides better performance regardless to the channel characteristics.

Finally, Figures 12 and 13 show the MSE and BER performances of the Sato and ABSato algorithms on Channel 5 with the fade rate fd=2 Hz. Figure 12 was the case of SNR=30 dB. While the division number $Q = 2$ was common, the step size and filter order were changed in Figures 12 and 13 as $\mu = 0.01$ and $M = 16$ in Figure 12 and $\mu = 0.001$ and $M = 5$ in Figure 13. Figures 12 and 13 indicate that even on time-variant channels, the ABSato algorithm provides an improvement.

Through all the above simulation results in this section, we see that the proposed ABSato algorithm provides better MSE and BER performances than the Sato

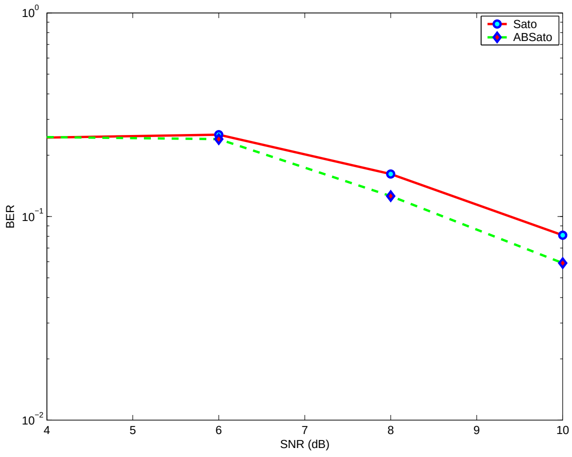

Fig. 11. BER performance of Sato and ABSato on Channel 4

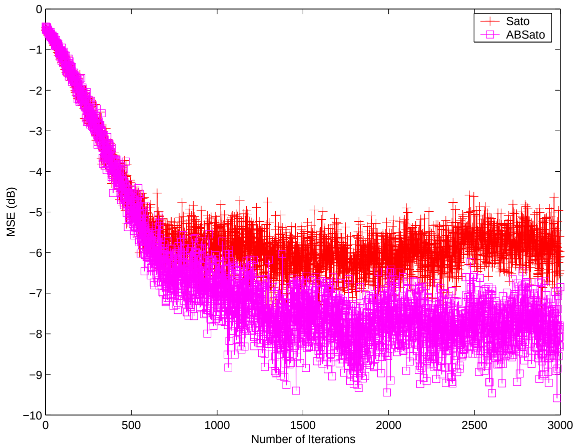

Fig. 12. MSE performance on Channel 5 with SNR=30 dB

algorithm for minimum phase, maximum phase, non-minimum phase and time-variant channels. This implies that the proposed ABSato algorithm is superior to the standard Sato algorithm for equalization of various types of channels. By looking at Figures 5, 6, 9 and 12 carefully, however, it is noticed that the convergence of the ABSato algorithm is slightly slower. This may be because the

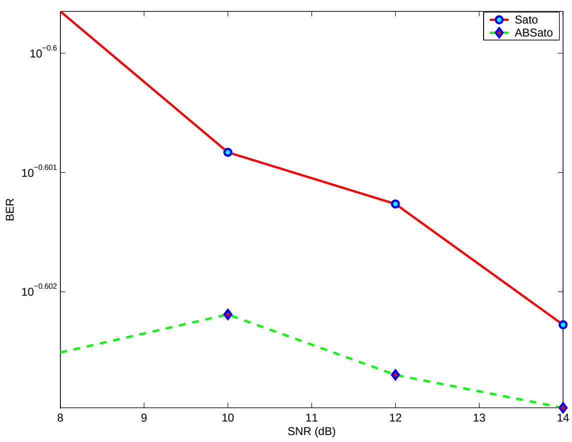

Fig. 13. BER performance of Sato and ABSato on Channel 5

number of coefficients to be updated for the ABSato algorithm is increased.

V. Filter Structure

To improve the performance of the ABSato algorithm, another filter structure is considered in this section.

A. Parallel Structure

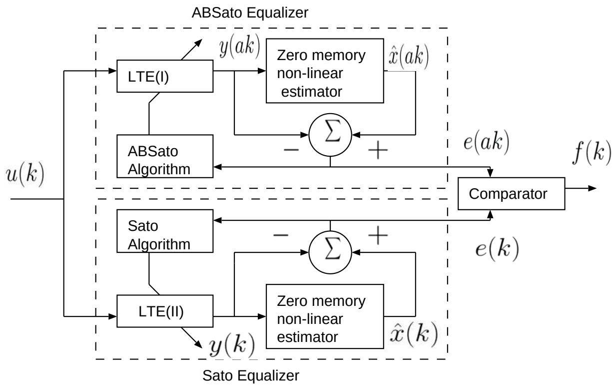

Fig. 14. Parallel Sato-ABSato equalizer

Figure 14 depicts a parallel structure of the Sato and ABSato equalizers. In the parallel structure, two linear transversal equalizers; LTE(I) and LTE(II), are updated by the ABSato and Sato algorithms with $e(ak)$ and $e(k)$, respectively. The comparator provides $f(k)$=$e(ak)$ if $(e(ak))^2 \leq (e(k))^2$ otherwise $f(k)$=$e(k)$. The parallel equalizer provides the output $y(ak)$ when $f(k)$=$e(ak)$ and $y(k)$ when $f(k) = e(k)$.

B. Performance Evaluation

The performances of the parallel Sato-ABSato equalizer were investigated on Channel 1. Figure 15 shows the MSE convergence plots of the Sato, ABSato and parallel Sato-ABSato equalizers with SNR=40 dB, M=8 and step size μ=0.025. The division number Q=4 was set for the ABSato algorithm. Figure 15 clarifies that the parallel structure of the Sato and ABSato algorithms provides better performance than non-parallel structure algorithms.

Figure 16 shows the BER performances of the Sato, ABSato and parallel Sato-ABSato algorithms with the filter order M=8 and step size μ=0.025. The division number Q=4 was set for the ABSato algorithm. Figure 16 suggests that even for BER, the parallel combination of the Sato and ABSato algorithms improves the performance. From Figures 15 and 16, we can confirm that the parallel structure enhances the performance of the ABSato algorithm with the support of the Sato algorithm.

Additionally we checked the performance of the parallel equalizer with the Godard and ABGodard algorithms, which is constructed in the same way as in Figure 14. The performance of the parallel Godard-ABGodard equalizer was, however, worse than that of the parallel Sato-ABSato equalizer. This result may be expected from those in Figures 5 and 6.

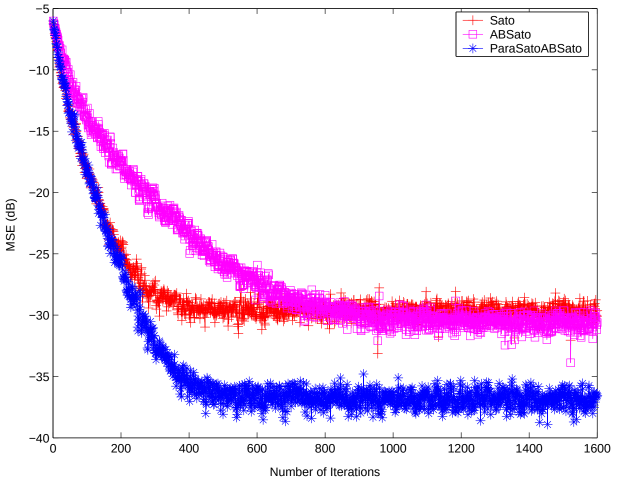

Fig. 15. MSE performance of Sato, ABSato and Parallel Sato-ABSato on Channel 1 with SNR=40 dB

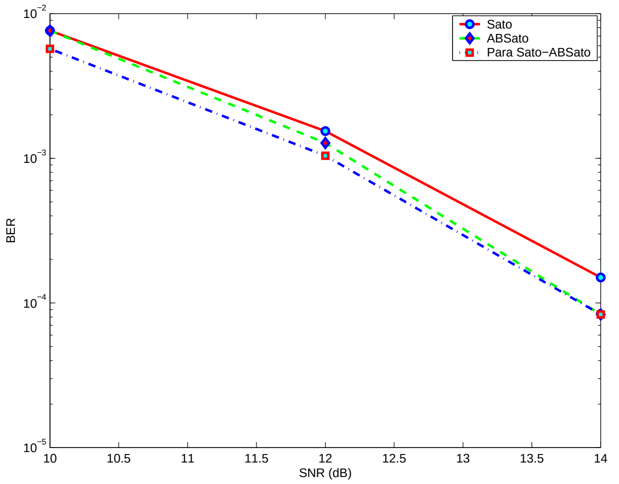

Fig. 16. BER performance of Sato, ABSato and Parallel Sato-ABSato on Channel 1

C. Performance Analysis

The reason why the parallel Sato-ABSato equalizer behaves better than the non-parallel Sato and ABSato equalizers is considered here.

Table II shows the subtotal values of the Sato equalizer error $e(k)$, ABSato equalizer error $e(ak)$ and parallel Sato-ABSato equalizer error $f(k)$ (which are denoted by $E_{(k)}$, $E_{(ak)}$ and $E_{(pak)}$, respectively) against an iteration range of 200. Table III shows the selection number of the equalizer errors $e(k)$ and $e(ak)$ in implementing the parallel Sato-ABSato equalizer, which are denoted by N_k and N_{ak}, respectively. Table II and III are investigations on Channel 1 being the same condition as in Figure 14, but one trial (no averaging). We have checked every datum at each iteration. However, to avoid difficulty of presenting a large number of data serially, we have considered an iteration-range based approach as shown in Tables II and III. Comparing with Figure 15, Tables II and III support to understand the function of the parallel Sato-ABSato equalizer. For iterations from 1 to 800, the subtotal error values of the Sato equalizer are less than those of the ABSato equalizer in Table II. This means that the parallel Sato-ABSato equalizer selects mostly the Sato equalizer error $e(k)$. The total selection number is 559 out of 800 as observed in Table II. On the other hand, for iterations from 801 to 1600, the parallel Sato-ABSato equalizer selects more the ABSato equalizer error $e(ak)$. The total selection number is 453. The parallel Sato-ABSato equalizer always selects the minimum equalizer error values. This property leads to acceleration of the convergence speed. Thus the parallel Sato-ABSato equalizer provide better performance than the non-parallel Sato and ABSato equalizers.

VI. Conclusion

In this paper, the ABGodard and ABSato algorithms have been proposed for blind channel equalization. Simulation results have demonstrated that the ABGodard and ABSato algorithms perform better than the Godard and Sato algorithms, respectively. The ABSato algorithm behaves more accurately than the ABGodard algorithm, and the increased division number leads to an improved performance of the ABSato algorithm. The use of a parallel structure enhances the performance of the ABSato algorithm further. Future work will aim at developing a transform-domain implementation technique of the proposed blind equalizer.

References

[1] S. U. H. Qureshi, "Adaptive equalization", Proc. IEEE, Vol.73, No.9, pp.1349-1387, 1982.

[2] A. Benveniste and M. Goursat, "Blind equalizers", IEEE Trans. Commun., Vol. COM-32, pp.871-882, Aug. 1982.

[3] D. N. Godard, "Self-recovering equalization and carrier tracking in two-dimensional data communication systems", IEEE Trans. Commun., Vol. Com-28, No.11, pp.1867-1875, Nov. 1980.

[4] Y. Sato, "A method of self-recovering equalization for multilevel amplitude modulation", IEEE Trans. Commun., Vol. COM-23, pp.679-682, June 1975.

[5] T. Shimamura and C. F. N. Cowan, "Equalization of time-variant multipath channels using amplitude banded LMS algorithms", IEICE Trans. Fundamentals on Electronics, Communications and Computer Sciences, Vol.E84-A, No.3, pp.802-812, 2001.

[6] T. Shimamura and C. F. N. Cowan, "Amplitude banded technique for time variant channel equalisation", Proc. IMA Int. Conf. Mathematics in Signal Processing, Dec. 1996.

[7] T. Shimamura, "Performance of the amplitude banded LMS equalizer on stationary channels", Proc. IEEE International Workshop on Nonlinear Dynamics of Electronic Systems, pp.289-292, 2007.

[8] S. Haykin, "Adaptive Filter Theory", Prentice-Hall, 1996.

[9] C. F. N. Cowan, "Channel equalization", in Adaptive System Identification and Signal Processing Algorithms, edited by N. Kaloutsidis and S. Theodoridis, Prentice-Hall, 1993.

[10] F. Ling and J. Proakis, "Adaptive lattice decision-feedback equalizers - their performance and application to time-variant multipath channelsh, IEEE Trans. Commun., Vol. COM-33, No. 4, pp.348-356, April 1985.

TABLE II
SUBTOTAL ERROR VALUES AGAINST ITERATIONS IN MSE PERFORMANCE

$IterationRange$	$1 \sim 200$	$201 \sim 400$	$401 \sim 600$	$601 \sim 800$	$801 \sim 1000$	$1001 \sim 1200$	$1201 \sim 1400$	$1401 \sim 1600$
E_k	7.73	0.39	0.22	0.23	0.19	0.18	0.27	0.19
E_{ak}	12.74	2.02	0.67	0.23	0.19	0.17	0.19	0.15
E_{pak}	7.54	0.21	0.06	0.05	0.04	0.03	0.04	0.04

TABLE III
SELECTION NUMBER OF ERROR VALUES OF SATO AND ABSATO ALGORITHMS AGAINST ITERATIONS IN MSE PERFORMANCE

$IterationRange$	$1 \sim 200$	$201 \sim 400$	$401 \sim 600$	$601 \sim 800$	$801 \sim 1000$	$1001 \sim 1200$	$1201 \sim 1400$	$1401 \sim 1600$
N_k	162	159	127	111	99	90	83	75
N_{ak}	38	41	73	89	101	110	117	125

Md. Lutfor Rahman. Khan received the B.Sc. (Hons) degree in Applied Physics and Electronics and M.Sc. degree in Computer Science from Dhaka University, Dhaka, Bangladesh, in 1996 and 1997, respectively. He is currently pursuing the Ph.D. degree at the Graduate School of Science and Engineering, Saitama University. His research area is involved with adaptive signal processing and its applications.

Md. H. Wondimagegnehu received the B.Sc. degree in Electrical Engineering from Faculty of Technology, Addis Ababa University, Addis Ababa, Ethiopia, in 1991, the Master of Engineering degree in Information Systems Engineering from, Graduate School of Science and Engineering, Saitama University, Saitama, Japan in 2004 and his Ph.D. degree in Information and Mathematical Sciences at the Graduate School of Science and Engineering, Saitama University, Saitama, Japan. His research activities include adaptive digital signal processing, muliti-channel signal processing, wireless and mobile digital signal processing as well as design of Field programmable group array devices using hardware development languages fo digital signal processing implementation. He is currently a Post-Doctoral Researcher in WSEAS.

Tetsuya. Shimamura received the B.E., M.E., and Ph.D. degrees in Electrical Engineering from Keio University, Yokohama, Japan, in 1986, 1988, and 1991, respectively. In 1991, he joined Saitama University, Saitama, Japan, where he is currently a Professor. He was a Visiting Scholar at Loughborough University (U.K.) in 1995 and at the Queen's University of Belfast (U.K.) in 1996, respectively. His interests are in digital signal processing and its applications to communication systems and speech processing. He is a member of IEEE, EURASIP, the Acoustical Society of Japan, and the Acoustical Society of America.